JOURNAL OF GEOPHYSICAL RESEARCH, VOL. ???, XXXX, DOI:10.1029/,

Local Partitioning of the Overturning Circulation in the Tropics and the Connection to the Hadley and Walker Circulation

Juliane Schwendike[1], Pallavi Govekar[1], Michael J. Reeder[1,2], Richard Wardle[3], Gareth J. Berry[1], and Christian Jakob[1,2]

Gareth J. Berry, (gareth.berry@monash.edu.au)

Pallavi Govekar, (pallavi.govekar@unimelb.edu.au)

Christian Jakob, (christian.jakob@monash.edu.au)

Michael J. Reeder, (michael.reeder@monash.edu.au)

Juliane Schwendike, (juliane.schwendike@monash.edu.au)

Richard M. Wardle, (r.wardle@bom.gov.au)

[1]Monash Weather and Climate, School of Mathematical Sciences, Monash University, VIC 3800 Australia.

[2]ARC Centre of Excellence for Climate System Science, Monash University, VIC 3800 Australia.

[3] Bureau of Meteorology, 69 Ann St., Brisbane, QLD 4000 Australia.

Abstract. Conceptually, it is useful to partition the three-dimensional tropical circulation into meridional and zonal components, namely the Hadley and Walker circulations. The averaging involved in their definitions can introduce ambiguities. These problems can be circumvented by first partitioning the total vertical mass flux into components associated with overturning in the meridional and zonal directions respectively, called here the local Hadley and local Walker circulations. Defining the local Hadley and local Walker circulations this way ensures the pair of two-dimensional overturning circulations can be added to give the original three-dimensional circulation, even when the averages are taken over limited domains. The method is applied to the vertical motion from the ERA-Interim reanalysis for the period 1979 to 2009. One important result is that the local Hadley circulation responds much more strongly to ENSO than the local Walker circulation, even though the local Walker circulation in the central Pacific weakens during El Niño years and strengthens and widens during La Niña years.

1. Introduction

Conceptually, it has proven to be very useful to partition the tropical atmosphere into two independent orthogonal overturning circulations. The first of these, the Hadley circulation, is commonly defined as the zonally-averaged circulation [e.g. *Hartmann*, 1994]. The second, the Walker circulation, represents the zonal asymmetries in the tropical circulation. The Walker circulation is often, but not always, defined by the meridional average of the tropical circulation [e.g. *Hartmann*, 1994], and its definition is often restricted to the tropical Pacific region [e.g. *Julian and Chervin*, 1978; *Vecchi et al.*, 2006; *Power and Smith*, 2007; *Tokinaga et al.*, 2012; *L'Heureux et al.*, 2013].

The Hadley circulation is thought of as the meridional response of the wind field to zonally-averaged net heating in the tropics. It plays a central role in our understanding of the energy and water budgets of the Earth [e.g. *Barry and Carleton*, 2001; *Trenberth and Stepaniak*, 2003]. Likewise, the Walker circulation is thought of as the zonal response of the wind field to zonal asymmetries in the meridionally-averaged net tropical heating. It is thought to be inextricably connected with the El Niño Southern Oscillation (ENSO), a connection often expressed through the Southern Oscillation Index (SOI). Both the Hadley and Walker circulations are closely connected to the Asian and Australian monsoons. The huge importance of the Hadley and Walker circulations in our description and understanding of weather and climate have motivated numerous studies on their dynamics [e.g. *Held and Hou*, 1980; *Gill*, 1980; *James*, 1994], their variability on interannual or interdecadal timescales [e.g. *Oort and Yienger*, 1996; *Chen et al.*, 2002; *Vecchi et al.*, 2006; *Yu and Zwiers*, 2010], and trends in their position and strength [e.g. *Quan et al.*, 2004; *Mitas and Clement*, 2005; *Zhao and Moore*, 2008; *Hu and Fu*, 2007; *Stachnik and Schumacher*, 2011], including possible changes under enhanced greenhouse conditions [e.g. *Lu et al.*, 2007; *Seidel et al.*, 2008; *Gastineau et al.*, 2009; *Kang and Lu*, 2012].

Although partitioning the tropical atmosphere into two orthogonal overturning circulations is qualitatively simple, it is more difficult quantitatively [*Tanaka et al.*, 2004; *Zhao and Moore*, 2008]. The main problem is that, in general, the two orthogonal overturning circulations are interconnected, as variations in the horizontal velocity in both the zonal and meridional directions contribute to the horizontal divergence. Consequently, part of the vertical motion is attributable to the circulation in zonal direction and part to that in the meridional direction. Unless the vertical motion is partitioned carefully, the orthogonal two-dimensional circulations need not sum to the original three-dimensional circulation. Resolving this ambiguity is especially important when assessing changes to the Hadley and Walker circulations. Thus, the main aim of the present paper is to provide a more rigorous basis for the common and useful practice of partitioning the three-dimensional tropical overturning circulation into its zonal and meridional components.

Keyser et al. [1989] have addressed the problem of partitioning three-dimensional circulations into orthogonal two-dimensional circulations. Their formalism is termed the "ψ-vector" method and has been applied to good effect in diagnosing the vertical circulations in mid-latitude baroclinic systems [*Keyser et al.*, 1989; *Reeder et al.*, 1991; *Keyser et al.*, 1992]. *Loughe et al.* [1995] have generalised the ψ-vector method to limited domains and conformal map projections. In the present work, a version of the ψ-vector method is used to partition the tropical atmosphere into Hadley and Walker circulations. With the requirement that the circulations in the two orthogonal vertical planes satisfy continuity independently, it is possible to uniquely attribute part of the vertical motion to the circulation in the zonal direction and part to that in the meridional direction. This approach ensures that the complete three-dimensional circulation is equal to the sum of the orthogonal two-dimensional circulations. The method will be used to define and examine the *local Hadley* and *local Walker circulations*. Furthermore, it will be shown that the approach is especially useful for defining regionally-averaged circulations.

The remainder of the paper is structured as follows. The method is outlined in Section 2. Section 3 discusses climatologies of the local Hadley and local Walker circulations. The anomalies that develop in association with El Niño and La Niña are presented in Section 4. This section examines also the relationship between these partitioned, orthogonal circulations and the more commonly used zonally and meridionally-averaged definitions of the Hadley and Walker circulations. Finally, the key conclusions of this study are summarised in Section 5.

2. Partitioning into zonal and meridional overturning circulations

This section describes the method by which the vertical motion, and hence, vertical mass flux is partitioned into zonal and meridional overturning circulations. It will be shown that the atmospheric vertical motion in pressure coordinates ω can be written as the sum of vertical motion associated with overturning in the zonal direction ω_λ, and vertical motion associated with overturning in the meridional direction ω_ϕ. The vertical mass fluxes associated with these two components will be referred to here as the *local Walker circulation* and the *local Hadley circulation* respectively, although the definitions are different from those used by other authors. For example, *Quan et al.* [2004] define the local circulations through an EOF analysis.

2.1. A variation of the ψ-vector method

The ψ-vector method developed by *Keyser et al.* [1989] is an objective method to partition a three-dimensional irrotational flow into a unique pair of orthogonal, two-dimensional circulations, with both satisfying continuity independently. *Keyser et al.* [1989], *Reeder et al.* [1991] and *Keyser et al.* [1992] applied this method to fronts and cyclones on an f-plane. In the present work, a variation of the ψ-vector method is reformulated in spherical coordinates and used to partition globally the vertical mass flux into zonal and meridional components (the local Walker and local Hadley circulations respectively).

The continuity equation in pressure coordinates is $\nabla_p^2 \chi + \partial\omega/\partial p = 0$, where p is the pressure, ∇_p is the gradient operator along a pressure surface, and χ is a velocity potential, which defines the divergent (irrotational) part of the horizontal wind through $\mathbf{u}_{div} = \nabla_p \chi$.

A potential function μ is defined such that $\chi = \partial\mu/\partial p$, which, when combined with the continuity equation, yields

$$\nabla_p^2 \mu = -\omega. \tag{1}$$

This expression is identical to the potential function defined by *Eliassen* [1962] and *Keyser et al.* [1989] (except the potential function μ is denoted χ in those studies). Equation (1) is a Poisson equation which can be solved for μ given suitable boundary conditions.

Defining now the vector stream function $\boldsymbol{\psi} = -\nabla_p \mu$ allows Eq. (1) to be written as

$$\nabla_p \cdot \boldsymbol{\psi} = \omega, \tag{2}$$

where $\boldsymbol{\psi}$ points towards (away from) regions of ascending (descending) motion. From the definitions of $\mathbf{u}_{div}$, χ, and $\boldsymbol{\psi}$, the divergent wind can be written in terms of the velocity streamfunction as

$$\mathbf{u}_{div} = (u_\lambda, u_\phi) = -\frac{\partial \boldsymbol{\psi}}{\partial p} = -\Big(\frac{\partial \psi_\lambda}{\partial p}, \frac{\partial \psi_\phi}{\partial p}\Big), \tag{3}$$

where u_λ and u_ϕ are the zonal and meridional components of the divergent part of the wind and ψ_λ and ψ_ϕ are the components of $\boldsymbol{\psi}$ in the zonal and meridional directions respectively.

From Eqs. (1), (2) and (3) the vertical motion can be partitioned into the zonal and meridional planes as

$$\omega_\lambda\, cos\phi = \frac{1}{a}\frac{\partial \psi_\lambda}{\partial \lambda} = \frac{1}{a^2\, cos\phi}\frac{\partial^2 \mu}{\partial \lambda^2}, \tag{4}$$

$$\omega_\phi\, cos\phi = \frac{1}{a}\frac{\partial}{\partial \phi}(\psi_\phi\, cos\phi) = \frac{1}{a^2}\frac{\partial}{\partial \phi}\left(cos\phi \frac{\partial \mu}{\partial \phi}\right), \tag{5}$$

where a is the radius of the Earth. Equations 3, 4 and 5 define two divergent circulations in orthogonal planes.

Continuity is satisfied independently in both the zonal and meridional directions since

$$\frac{1}{a}\frac{\partial u_\lambda}{\partial \lambda} + \frac{\partial}{\partial p}(\omega_\lambda\, cos\phi) = 0,$$

$$\frac{1}{a}\frac{\partial}{\partial \phi}(u_\phi\, cos\phi) + \frac{\partial}{\partial p}(\omega_\phi\, cos\phi) = 0$$

and consequently the vertical integral of the horizontal mass flux vanishes independently in each orthogonal vertical plane. The vertical motion is the sum of the vertical motion partitioned in the two orthogonal directions $\omega = \omega_\lambda + \omega_\phi$, and the upward mass fluxes associated with the zonal and meridional parts of the circulation are

$$m_\lambda = -\omega_\lambda\, cos\phi/g \qquad \text{and} \qquad m_\phi = -\omega_\phi\, cos\phi/g \tag{6}$$

respectively, where g is the gravitational acceleration.

Partitioning the three-dimensional overturning circulation into a pair of two-dimensional overturning circulations $(u_\lambda, \omega_\lambda)$ and (u_ϕ, ω_ϕ) is conceptually useful, objective, unambiguous, and especially beneficial if the circulations are averaged over a limited area as will be shown later. In the plots that follow the two-dimensional local Hadley circulation is portrayed by the vertical mass flux m_ϕ and the divergent part of the circulation in the meridional plane (u_ϕ, ω_ϕ). Likewise, the local Walker circulation is portrayed by the vertical mass flux m_λ and the divergent circulation in the zonal plane $(u_\lambda, \omega_\lambda)$.

Note that the formulation outlined above is different from the ψ-vector method described by *Keyser et al.* [1989]. In the original formulation the horizontal wind is first decomposed into its geostrophic and ageostrophic components $\mathbf{u}_h = \mathbf{u}_g + \mathbf{u}_{ag}$, and then each component is subdivided into its rotational $(\mathbf{u}_{g,rot}, \mathbf{u}_{ag,rot})$ and irrotational (divergent; $\mathbf{u}_{g,irr}, \mathbf{u}_{ag,irr}$) parts. (Here the terms rotational and nondivergent are used interchangeably as are the terms irrotational and divergent.) As the geostrophic wind is nondivergent, the irrotational component of the geostrophic wind vanishes and the irrotational part of the horizontal velocity is given only by the ageostrophic component. Hence, *Keyser et al.* [1989] write the horizontal wind as $\mathbf{u}_h = \mathbf{u}_{g,rot} + \mathbf{u}_{ag,rot} + \mathbf{u}_{ag,irr}$. In the present work, the horizontal wind is not separated into its geostrophic and ageostrophic components as the method is applied to circulations in the tropics. The horizontal wind is separated only into its rotational and irrotational components $\mathbf{u}_h = \mathbf{u}_{irr} + \mathbf{u}_{rot}$, which can be rewritten as $\mathbf{u}_h = -\nabla_p(\partial\mu/\partial p) + \mathbf{k} \times \nabla_p\, s$, where $(\partial\mu/\partial p)$ is the potential function, $\mathbf{k}$ is the unit vector in the vertical and s is a stream function. Helmholtz's theorem tells us that this decomposition is unique on a sphere.

Indices closely related to the local zonal and local meridional overturning circulations have been used previously in studies of the Asian monsoon [*Webster and Yang*, 1992; *Oort and Yienger*, 1996; *Goswami et al.*, 1999] and the Hadley and Walker circulations [*Moore et al.*, 2004]. These indices, called the *Zonal Overturning Index* (ZOI) and *Meridional Overturning Index* (MOI) by *Moore et al.* [2004], are defined by the difference in the divergent part of the zonal and meridional winds at 200 hPa and 850 hPa, the expressions for which are $ZOI = u_{\lambda 200} - u_{\lambda 850}$ and $MOI = u_{\phi 200} - u_{\phi 850}$. The ZOI and MOI are related to the components of the ψ-vector, but will not be used here. For reference, $ZOI = \partial(\psi_{\lambda 200} - \psi_{\lambda 850})/\partial p$ and $MOI = \partial(\psi_{\phi 200} - \psi_{\phi 850})/\partial p$ (using Eq. (3)). Replacing the vertical derivative with a simple finite difference approximation, using Eqs. (4) and (5), and assuming the vertical motion at 850 and 200 hPa is small compared with that at 525 hPa (the center of the layer), gives $m_{\lambda 525} = -\delta p/(2ag)\partial(ZOI)/\partial\lambda$ and $m_{\phi 525} = -\delta p/(2ag\, cos\phi)\partial(MOI\, cos\phi)/\partial\phi$ where $\delta p = 200 - 850$ hPa. With these assumptions, the local Walker and local Hadley circulations are proportional to the zonal gradient of the ZOI and the meridional gradient of the MOI respectively.

To conclude this section we note that several other studies have examined the zonal and meridional overturning circulations using the divergent part of the wind; these include *Yu and Zwiers* [2010], *Hagos and Zhang* [2010], and *Hagos and Leung* [2012]. However, only the present study shows how to decompose the divergent flow into two unique, orthogonal circulations that sum up to the original divergent flow filed.

2.2. Zonal and meridional averaging over restricted intervals

This section examines the relationship between the averaged overturning circulations and the local overturning circulations, which are part of the definitions of the Hadley and Walker circulations. Of course, averaging in meridional and zonal direction obscures the highly regional nature of the local Hadley and local Walker circulations.

The *Hadley circulation* (as distinct from the local Hadley circulation) is defined as the zonally-averaged circulation, where the average is taken around an entire circle of constant latitude. The zonally-averaged mass flux is $[m]_{\lambda_1}^{\lambda_2} = [m_\lambda]_{\lambda_1}^{\lambda_2} + [m_\phi]_{\lambda_1}^{\lambda_2}$, where the averaging operator is

$$[A]_{\lambda_1}^{\lambda_2} = \frac{1}{\Delta\lambda}\int\limits_{\lambda_1}^{\lambda_2} A\, d\lambda. \tag{7}$$

Here, A is any given variable, λ_1 and λ_2 are the initial and final longitudes and $\Delta\lambda = \lambda_2 - \lambda_1$. In particular, $[m_\lambda]_{\lambda_1}^{\lambda_2} = -(\psi_\lambda|_{\lambda_2} - \psi_\lambda|_{\lambda_1})/(ag\Delta\lambda cos\,\phi)$, a result which follows from the zonal average of Eqs. 4 and 5. In general, ψ_λ is small compared with ψ_ϕ and, for this reason, $[m_\lambda]_{\lambda_1}^{\lambda_2}$ is small compared with $[m_\phi]_{\lambda_1}^{\lambda_2}$ even when the averaging is defined on a limited domain (see later Section 3.2).

That the relative smallness of $[m_\lambda]_{\lambda_1}^{\lambda_2}$ is a consequence of the geometry of the sea surface temperature anomalies driving convection in the tropics can be illustrated by estimating the ratio between ω_λ and ω_ϕ under the assumption that $cos\,\phi$ is almost one near the equator, in which case equations 4 and 5 give $|\omega_\lambda/\omega_\phi| = |(\partial^2\mu/\partial\lambda^2)/(\partial^2\mu/\partial\phi^2)| \approx (\Delta\phi/\Delta\lambda)^2$. Considering now the typical dimensions of the tongue of anomalously cool or anomalously warm water in the eastern Pacific during ENSO events, $\Delta\phi$ is of order 30 degrees and $\Delta\lambda$ is of order 100 degrees. In this case, $|\omega_\lambda/\omega_\phi| \approx 0.1$. This simple scale analysis shows that ω_λ is about one order of magnitude smaller than ω_ϕ.

When averaging around an entire latitude circle we omit the terminals λ_2 and λ_1, simplifying the notation to $[A]$. As $\lambda_2 = \lambda_1 + 2\pi$, $[m_\lambda] = 0$, and hence $[m] = [m_\phi]$, which is consistent with previous definitions of the Hadley circulation. Of course, $[m_\lambda]_{\lambda_1}^{\lambda_2}$ need not vanish when the averaging operator is defined over a restricted domain. In this case, the average mass flux $[m]_{\lambda_1}^{\lambda_2}$ includes contributions from both ψ_λ and ψ_ϕ, which complicates the interpretation of the average circulation defined this way.

For reference, the commonly used mass-weighted meridional streamfunction [e.g. *Hartmann*, 1994] denoted here Ψ_ϕ, is related to the meridional component of the ψ-vector through the expression $\Psi_\phi = -(2\pi a \, cos\,\phi/g)[\psi_\phi]$, where the zonal average is taken from 0 to 2π.

The *Walker circulation* (as distinct from the local Walker circulation) is defined as the meridionally-averaged circulation, although in this case it is common to restrict the averaging interval to the low latitudes. The meridional average of the mass flux is $< m >_{\phi_1}^{\phi_2} = < m_\lambda >_{\phi_1}^{\phi_2} + < m_\phi >_{\phi_1}^{\phi_2}$, where the averaging operator is now

$$< A >_{\phi_1}^{\phi_2} = \frac{1}{\Delta\phi} \int_{\phi_1}^{\phi_2} A \, cos\,\phi \, d\phi. \tag{8}$$

Here ϕ_1 and ϕ_2 are the initial and final latitudes and $\Delta\phi = \phi_2 - \phi_1$. Specifically, $< m_\phi >_{\phi_1}^{\phi_2} = -(cos\,\phi\,\psi_\phi|_{\phi_2} - cos\,\phi\,\psi_\phi|_{\phi_1})/(ag\Delta\phi)$, which vanishes when $\phi_2 = \pi/2$ and $\phi_1 = -\pi/2$, but is non-zero otherwise. It follows that when the Walker circulation is defined over a restricted latitude band, the vertical mass flux includes a contribution from the meridional circulation through the terms involving ψ_ϕ. In general, ψ_ϕ cannot be neglected and, hence, $< m_\phi >_{\phi_1}^{\phi_2}$ makes a large, even dominant, contribution when averaging on a limited domain (see Section 3.2).

For reference only, the relationship between the zonal component of the ψ-vector and the mass-weighted zonal streamfunction [e.g. *Hartmann*, 1994] is $\Psi_\lambda = -(\pi a/g) < \psi_\lambda >$, where Ψ_λ is the mass-weighted zonal streamfunction and the meridional average is taken from $-\pi/2$ to $\pi/2$.

Henceforce, the meridional overturning circulation at a point or in a plane will be termed the *local Hadley circulation*, and the zonal overturning circulation at a point or in a plane will be termed the *local Waker circulation.* When the meridional overturning circulation and the zonal overturning circulations are averaged over an area, they will be referred to as *regional Hadley* and *regional Walker circulations*, respectively.

The regional Hadley (the zonally-averaged local Hadley circulation) and the regional Walker (meridionally-averaged local Walker circulation) circulations are defined as $[m_\phi]_{\lambda_1}^{\lambda_2}$ and $< m_\lambda >_{\phi_1}^{\phi_2}$, respectively, where (λ_1, λ_2) and (ϕ_1, ϕ_2) are arbitrary. The zonally-averaged mass flux $[m]_{\lambda_1}^{\lambda_2} = [m_\phi]_{\lambda_1}^{\lambda_2} + [m_\lambda]_{\lambda_1}^{\lambda_2}$ also includes a contribution from the zonal overturning circulation $[m_\lambda]_{\lambda_1}^{\lambda_2}$. Likewise, the contribution from the meridional overturning circulation to the meridionally-averaged mass flux $< m >_{\phi_1}^{\phi_2} =< m_\phi >_{\phi_1}^{\phi_2} + < m_\lambda >_{\phi_1}^{\phi_2}$, is $< m_\phi >_{\phi_1}^{\phi_2}$.

3. Local Hadley and local Walker circulations

In this section the local Hadley circulation and the local Walker circulation are diagnosed from the ERA-Interim reanalysis [*Simmons et al.*, 2011; *Dee et al.*, 2011] with a horizontal resolution of 1.5 degrees and 37 vertical pressure levels for the period from 1979 to 2009.

3.1. Global climatology

The time-mean local Hadley and local Walker circulations as defined by the meridional and zonal mass fluxes at 500 hPa are shown in Figs. 1 and 2, respectively, for December, January, February (DJF) and June, July, August (JJA). The present study is not the first to characterize the Hadley and Walker circulations by the vertical motion [e.g. *Kumar et al.*, 1999; *Trenberth et al.*, 2000; *Wang*, 2002; *Tanaka et al.*, 2004], although it is the first to partition the vertical motion and attribute specific parts to the Hadley and Walker circulations.

In both seasons, the local Hadley circulation (Fig. 1) is characterized by zonally-elongated bands of vertical mass flux, with ascent prominent in the tropics and subsidence prominent in the subtropics, reflecting the mean rainfall (not shown). The ascent is shifted towards the summer hemisphere and the subsidence is more marked in the winter hemisphere. The main exception to this picture is in the equatorial eastern Pacific, where there is subsidence along the equator, extending southwards into the extratropics. The region is bounded to the north by a band of strong ascent marking the Inter-Tropical Convergence Zone (ITCZ) there.

In contrast to the time-mean local Hadley circulation, the bands of vertical mass flux comprising the time-mean local Walker circulation are mostly oriented meridionally (Fig. 2). Moreover, almost everywhere, the time-mean local Walker circulation is weaker, and its seasonal variation smaller, than the corresponding time-mean local Hadley circulation.

During Southern Hemisphere summer (DJF), the time-mean local Walker circulation (Fig. 2a) is most pronounced on the western sides on the Southern Hemisphere continents. The local Walker circulation is strongest in the eastern Pacific and South America, with ascent over the continent and subsidence over the adjacent ocean. Similarly, there are pronounced bands of subsidence over the Atlantic to the west of Africa, and over the Indian Ocean to the West of Australia. These bands of subsidence are accompanied by ascent of the western side of southern Africa and western Australia. A pattern of alternating ascent and subsidence, most likely a consequence of the underlying orography, is located over the Rockies, the Middle East and Asia.

The time-mean local Walker circulation in JJA (Fig. 2b) is more pronounced in the Northern Hemisphere. Centers of ascent are located in the Bay of Bengal and to its north, and over the south Pacific. Bands of ascent also lie along the eastern side of the north Pacific and through much of the Americas and the Caribbean. Notable centers of subsidence lie over the eastern Mediterranean Sea, over Somalia and the western Indian Ocean, to the east of the Caspian Sea, and off the west coast of the United States. Strong bands of ascent and subsidence lie along the Andes.

Vertical cross sections through the Hadley circulation $[m_\phi]$ (zonally-averaged around the whole globe) are shown in Fig. 3. Also plotted is the divergent circulation in the plane of the cross section ($[u_\phi], [\omega_\phi]$). In both seasons the Hadley circulation comprises an ascending branch to the summer side of the equator accompanied by descending branches to the north and south. The branch in the winter hemisphere is more pronounced than that in the summer hemisphere. In JJA the downward mass flux in the Northern Hemisphere is extremely weak effectively making the Hadley circulation single cell [*James*, 1994]. The ascending branch of the Hadley circulation is wider and weaker during DJF and narrower and more intense during JJA. As mentioned in Section 2.2, the contribution of the zonal overturning circulation $[m_\lambda]$ vanishes when averaged zonally around the globe giving the textbook picture of the Hadley circulation [e.g. *Hartmann*, 1994; *James*, 1994].

3.2. Regional climatology

The principle advantage of identifying the local Hadley and local Walker circulations through the ψ-vector method is that it leads to a simple unambiguous way to calculate regional circulations. As an illustration, the regional Hadley circulation over the Maritime Continent (zonally-averaged between 110°E and 160°E; box in Fig. 1) $[m_\phi]_{110^\circ E}^{160^\circ E}$ and the regional Walker circulation (meridionally-averaged between 10°N and 35°S; box in Fig. 2) $< m_\lambda >_{35^\circ S}^{10^\circ N}$ are examined. The latter region is somewhat different from that typically used to define the Walker circulation (e. g. 5°N to 5°S, which is sometimes referred to as the equatorial Walker circulation [e.g. *Bell and Halpert*, 1998; *Webster and Yang*, 1992], or 10°N-10°S [e.g. *L'Heureux et al.*, 2013; *Krishnamurthy and Goswami*, 2000]). In the following, both $< m_\lambda >_{35^\circ S}^{10^\circ N}$ and $< m_\lambda >_{5^\circ S}^{5^\circ N}$ are compared. The latitudinal interval from 10°N to 35°S is chosen because the maxima of the upward and downward zonal mass flux lie in this band.

The regional Hadley circulation over the Maritime Continent $[m_\phi]_{110^\circ E}^{160^\circ E}$ (Fig. 4) is different to the Hadley circulation $[m_\phi]$ (Fig. 3). A clear double cell structure is found in DJF (Fig. 4a), whereas in JJA (Fig. 4b) the single cell structure is apparent with the largest downward mass flux mainly in the midlatitudes. In contrast to the Hadley circulation (Fig. 3), the ascending branch of the regional Hadley circulation is broader in JJA than during DJF. The descending branch in the winter hemisphere is more pronounced than in the summer hemisphere. In JJA the descending branch comprises two maxima (see also Fig. 1), the more southward associated with the descending branch of the regional Hadley circulation and the more northward is associated with the South Pacific convergence zone (SPCZ). These plots capture the annual shift in the position of the Hadley circulation and the influence of the Asian monsoon (JJA) and the Australian monsoon (DJF).

Figure 4c, d displays the contribution to the regional Hadley circulation from the zonal overturning circulation $[m_\lambda]_{110^\circ E}^{160^\circ E}$. This contribution is the difference between the zonally-averaged mass flux $[m]_{110^\circ E}^{160^\circ E}$ and the regionally-averaged Hadley circulation $[m_\phi]_{110^\circ E}^{160^\circ E}$, and it represents the error in attributing the circulation to a regionally-averaged meridionally overturning circulation. In DJF the zonal overturning circulation contributes to the ascent south of about 20°N and to the descent north of this latitude. In JJA there is a distinct contribution from the zonal overturning circulation to the upward vertical mass flux. Overall, however, the contribution from the zonal overturning circulation to the regional Hadley circulation is relatively small because the zonal overturning circulation itself is small. In contrast, as discussed below, the meridional overturning circulation contributes significantly to the regional Walker circulation, which is large compared to the meridionally-averaged mass flux (see the scale analysis in section 2.2).

Figure 5 shows the regional Walker circulation defined by the latitudinal band [35°S, 10°N]. The three fields plotted are the regional Walker circulation $< m_\lambda >_{35^\circ S}^{10^\circ N}$, the contribution to the circulation from the meridional overturning circulation $< m_\phi >_{35^\circ S}^{10^\circ N}$, and the sum $< m_\lambda >_{35^\circ S}^{10^\circ N} + < m_\phi >_{35^\circ S}^{10^\circ N} = < m >_{35^\circ S}^{10^\circ N}$, which is the meridionally-averaged mass flux. Throughout the year three distinct cells comprise the regional Walker circulation $< m_\lambda >_{35^\circ S}^{10^\circ N}$: one in the Indian Ocean, one in the Pacific Ocean and one in the Atlantic (see the first row in Fig. 5). Also shown is the divergent circulation $(< u_\lambda >_{35^\circ S}^{10^\circ N}, < \omega_\lambda >_{35^\circ S}^{10^\circ N})$ attributable to the regional Walker circulation. The regional Walker circulation in the

Pacific is the largest of the three, with ascent over the Maritime Continent and western Pacific Ocean and descent in the eastern Pacific. In DJF the cell in the Pacific is very pronounced and the descent in the eastern Pacific Ocean is particularly strong. The regional Walker circulation in the Atlantic is intense but much narrower, whereas the regional Walker circulation in the Indian Ocean is relatively weak and most pronounced at the west coast of Australia. In contrast, in JJA, the regional Walker circulation in the Indian Ocean is much stronger and broader. The regional Walker circulation in the Atlantic is weaker and the ascending branch of the Pacific cell is more distinct than the descending branch.

The second row of Fig. 5 shows the meridionally-averaged mass flux $< m >_{35^\circ S}^{10^\circ N}$ and the wind field $(< u_\lambda >_{35^\circ S}^{10^\circ N}, < \omega >_{35^\circ S}^{10^\circ N})$. This is the circulation that results from simple averaging. The differences between $< m_\lambda >_{35^\circ S}^{10^\circ N}$ and $< m >_{35^\circ S}^{10^\circ N}$ are shown in the third row of Fig. 5. This difference quantifies the contribution from the meridional overturning circulation $< m_\phi >_{35^\circ S}^{10^\circ N}$ and is the error in the regional Walker circulation when it is identified with the mass flux $< m >_{35^\circ S}^{10^\circ N}$. In DJF there is a large positive contribution from $< m_\phi >_{35^\circ S}^{10^\circ N}$ to $< m >_{35^\circ S}^{10^\circ N}$ over the Maritime Continent and the western Pacific as well as over South America, which means that the values of $< m_\phi >_{35^\circ S}^{10^\circ N}$ reach up to 50% of the values of $< m >_{35^\circ S}^{10^\circ N}$. Over the Maritime Continent, in particular, $< m_\phi >_{35^\circ S}^{10^\circ N}$ is larger than $< m_\lambda >_{35^\circ S}^{10^\circ N}$. In JJA the contribution of $< m_\phi >_{35^\circ S}^{10^\circ N}$ to the meridionally-averaged downward vertical mass flux is large also. Here $< m_\phi >_{35^\circ S}^{10^\circ N}$ is up to one third of $< m >_{35^\circ S}^{10^\circ N}$. Figure 5 underscores the point that partitioning the tropical circulation into two orthogonal circulations is qualitatively simple but quantitatively less so. Simple averaging over a restricted band of latitudes leads to a resulting meridionally-averaged mass flux $< m >_{35^{\circ}S}^{10^{\circ}N}$ and circulation that are too strong, as part of the vertical mass flux should be attributed to the meridional overturning circulation, especially over the Maritime Continent and the Western Pacific. The reason for this is that the local Walker circulations are relatively weak compared to the local Hadley circulations.

It is common to define the regional Walker circulation as a meridional average between 5°S and 5°N [e.g. *Bell and Halpert*, 1998; *Webster and Yang*, 1992] (see Fig. 6). In this case the regional Walker circulation $< m_{\phi} >_{5^{\circ}S}^{5^{\circ}N}$ (Fig. 6a, b) is slightly different to that based on averaging between 35°S to 10°N $< m_{\phi} >_{35^{\circ}S}^{10^{\circ}N}$ (Fig. 5a, b), although the essential characteristics of the regional Walker circulations remain the same. However, the differences between $< m_{\lambda} >_{5^{\circ}S}^{5^{\circ}N}$ and $< m >_{5^{\circ}S}^{5^{\circ}N}$ (Fig. 6c, d) are striking. Figure 6e, f shows the contribution of the meridional overturning circulation $< m_{\phi} >_{5^{\circ}S}^{5^{\circ}N}$ to the zonally-averaged mass flux $< m >_{5^{\circ}S}^{5^{\circ}N}$. The vertical mass flux is so strong partly because this region lies in the ascending branch of the regional Hadley circulation, while the previous region (35°S and 10°N) was much broader and thus also contained parts of the descending branches of the regional Hadley circulation leading to some cancelation. Nevertheless, the contribution of the meridional overturning circulation in the band between 5°S and 5°N is much stronger than in the band ranging from 35°S to 10°N. This indicates that, not only is a careful partitioning of the vertical mass flux important, but the position of the domain over which the average is taken affects the result.

4. ENSO and the local Hadley and local Walker circulations

The previous section showed that the partitioning of the vertical velocity and, hence, the vertical mass flux can be achieved in an objective and unambiguous way using the ψ-vector method. This method can be applied to a variety of problems, a particularly interesting one being variations in the local Hadley and local Walker circulations with ENSO, the largest mode of variability in the Pacific region.

In this section anomalies from the local Hadley and local Walker circulation climatology are calculated for periods of El Niño and La Niña. To do so, first the time series of the Southern Oscillation index (SOI), which was obtained from Australian Bureau of Meteorology (ftp://ftp.bom.gov.au/anon/home/ncc/www/sco/soi/soiplaintext.html), was smoothed using a three months running average. The smoothed SOI of ± 0.9 standard deviation was used to separate the ERAI data into El Niño (47 months), La Niña (51 months) and neutral (274 months) periods. Then seasonal averages were taken over these periods. In the following we focuss on the El Niño and La Niña phases.

4.1. Global ENSO climatology

Figures 7 and 8 show the mean anomalies at 500 hPa in the local Hadley and local Walker circulations in DJF and JJA for El Niño and La Niña periods, respectively. During El Niño events in DJF (Fig. 7a), the local Hadley circulation has a pronounced anomaly in the ascent over the central Pacific, with strong anomalies in the subsidence to the north and south of the ascent anomaly. There is a strong subsidence anomaly over the Maritime Continent, weakening the mean ascent in that region (Fig. 1a). The subsidence anomaly extends southeastward from the Maritime Continent across the South Pacific. In contrast, during La Niña events (Fig. 7b), the ascent in the local Hadley circulation inceases over the Maritime Continent and South Pacific (Fig. 1a). The response over the central Pacific is both weaker and of the opposite sign to that during an El Niño. During El Niño events in JJA (Fig. 7c) there is also a positive anomaly over the central Pacific. The negative anomalies north and south of it are much weaker than in DJF. There is a band of anomalous ascent across the Pacific islands. To the west of this band the subsidence is enhanced. In JJA during La Niña, the signs of the anomalies are reversed and the anomalies are generally weaker (Fig. 7d).

The main response of the local Walker circulation to an El Niño is a meridional band of anomalous ascent in the central Pacific extending north and south along the eastern margin of the basin (Fig. 8a). There are more confined bands of anomalous ascent running from the Indian Ocean to the Middle East. A prominent band of anomalous subsidence runs from the Maritime Continent both northwest to the western part of the north Pacific, and southeast across Australia and the South Pacific. The response of the local Walker circulation to a La Niña is less coherent than the response to an El Niño (Fig. 8b). There is generally anomalous ascent across the Maritime Continent, as well as the regions north and south of it, anomalous ascent in the Southwest Pacific, and anomalous subsidence in the longitudes of India as well as in the Central Pacific. Thus, in agreement with *Oort and Yienger* [1996], the local Walker circulation weakens during El Niño years and strengthens during La Niña years. In JJA during an El Niño (Fig. 8c), the distribution of the anomalies is very similar to that in DJF, although less coherent. There is an ascent anomaly in the central Pacific and a descent anomaly along the coast of South America and across the Maritime Continent. During a La Niña the picture of the local Walker circulation in the Pacific is less clear (Fig. 8d). A band of anomalous descent lies along the western Pacific in both hemispheres and a band of anomalous ascent in the Bay of Bengal, over the Maritime Continent, and along the South American coastline.

Perhaps the key point to emerge from this analysis is that the local Hadley circulation responds more strongly to an El Niño than the local Walker circulation. The probable reason for this difference in the response is that that region of warm sea water that drives the El Niño is zonally elongated and, consequently, the temperature gradients in the meridional direction are larger than those in the zonal direction. This interpretation is consistent with the scale analysis given in Section 2.2. Hence, the ψ-vector approach provides a viewpoint different from many introductory textbooks which portray ENSO as a change in the Walker circulation. From this perspective, ENSO should not be portrayed as a shift in the Walker circulation, but rather, a change in the Hadley circulation. Nonetheless, in the central and eastern Pacific, the local Walker circulation is strengthened during a La Niña and weakened during an El Niño.

4.2. Regional Hadley circulation

The regional Hadley circulation response to ENSO over the Maritime Continent $[m_\phi]_{110^\circ E}^{160^\circ E}$ is shown in Fig. 9a, b. In DJF during both El Niño and La Niña periods the regional Hadley circulation has a typical two cell structure with ascent along the ITCZ and descent on each side, with the winter cell being stronger. The ascending branch of the regional Hadley circulation is stronger and wider during La Niña consistent with increased convection. The extent of the descending branches is the same in both periods. The descending branch in the Northern Hemisphere shows marked differences. During El Niño the descent is weaker and the maximum occurs at around 40°N. During La Niña, this maximum in descent is stronger and a second maximum occurs at about 20°N and at higher levels.

The zonally-averaged mass flux $[m]_{110^\circ E}^{160^\circ E}$ shows a very similar structure (Fig. 9c, d) to the regional Hadley circulation. The differences between circulations are small, as shown in

Fig. 9e, f which displays the contribution from the zonal overturning circulation $[m_\lambda]_{110^\circ E}^{160^\circ E}$. It is apparent that $[m_\lambda]_{110^\circ E}^{160^\circ E}$ is much smaller that $[m_\phi]_{110^\circ E}^{160^\circ E}$.

In JJA, the regional Hadley circulation over the Maritime Continent $[m_\phi]_{110^\circ E}^{160^\circ E}$ is characterized by a single cell structure. In contrast to DJF, the main ascent is located in the same region during El Niño and La Niña periods, but is slightly stronger during El Niño (Fig. 10a, b). The mid-latitude Ferrel cell in the summer hemisphere is due to averaging on isobaric levels (see *Holton* [2004]). In the winter hemisphere during El Niño there are two maxima in the descending branch of the regional Hadley circulation located close to one another. During La Niña, however, the two maxima in descent are more distinct. The equatorward maximum is related to the SPCZ whereas the poleward maximum is related to the descending branch of the regional Hadley circulation. The contribution from the zonal overturning circulation $[m_\lambda]_{110^\circ E}^{160^\circ E}$ (Fig. 10e, f) to the zonally-averaged mass flux $[m]_{110^\circ E}^{160^\circ E}$ (Fig. 10c, d) is mainly positive throughout the whole domain, with its maximum in the region of ascent of the regional Hadley circulation. However, as in DJF, the contribution from the zonal overturning circulation is much smaller than the regional Hadley circulation, which results in a close resemblance of $[m_\phi]_{110^\circ E}^{160^\circ E}$ to $[m]_{110^\circ E}^{160^\circ E}$.

4.3. Regional Walker circulations

Vertical cross-sections through the regional Walker circulations, defined by a meridional average from 35°S to 10°N (as in Fig. 2), for DJF during El Niño and La Niña are shown in Fig. 11a, b. During El Niño the strongest ascent occurs in the central Pacific with the descending branch of the regional Walker circulation located in the eastern Pacific. The regional Walker circulation in the Atlantic is much narrower although the ascent is comparable in strength to that over the central Pacific. The maximum ascent occurs over the eastern part of South America which is accompanied by descent in the eastern Atlantic. The regional Walker circulation in the Indian Ocean is the weakest. During La Niña, the maximum ascent in the Pacific moves westward and is located over the western Pacific and the Maritime Continent although the magnitude remains unchanged. The accompanying descent in the eastern Pacific increases and the regional Walker circulation in the Pacific becomes broader. The area of descent in the Indian Ocean extends westwards, and the descent west of Australia is stronger. Moreover, the regional Walker circulation in the Atlantic strengthens, but does not change position.

The Walker circulation based on the meridionally-averaged mass flux $< m >_{35^\circ S}^{10^\circ N}$ is much stronger than the regional Walker circulation $< m_\lambda >_{35^\circ S}^{10^\circ N}$ (Fig. 11c, d). The contribution from the meridional overturning circulation $< m_\phi >_{35^\circ S}^{10^\circ N}$ is shown in Fig. 11e, f. It is particularly strong in the central Pacific and over South America during El Niño and over the Maritime Continent and South America during La Niña. The Walker circulation based on the divergent circulation has ascent over the Indian Ocean when the regional Walker circulation has descent because of the effect of the meridional overturning circulation.

The differences in the Walker circulation and the regional Walker circulation are even more dramatic when a merdional average between 5°S and 5°N is used (not shown). The meridionally-averaged mass flux $< m >_{5^\circ S}^{5^\circ N}$ is too strong everywhere as the contribution from the meridional overturning circulation $< m_\phi >_{5^\circ S}^{5^\circ N}$ is large, particularly in the regions of ascent. Note, however, that the meridional overturning circulation averaged between 5°S and 5°N, $< m_\lambda >_{5^\circ S}^{5^\circ N}$, and 35°S and 10°N, $< m_\lambda >_{35^\circ S}^{10^\circ N}$, provide very similar pictures.

The regional Walker circulations are generally weaker in JJA than in DJF (not shown). During El Niño the regional Walker circulation in the Indian Ocean is the strongest whereas those in the Pacific region and in the Atlantic are relatively weak. During La Niña, the region of ascent in the western Pacific and over the Maritime Continent remains in the same location as in DJF but intensifies, leading to a stronger regional Walker circulation in the Indian Ocean and in the Pacific. However, the regional Walker circulation in the Indian Ocean is still the most distinct. As in DJF, the meridionally-averaged mass flux produces a much stronger regional Walker circulation. The contribution from the meridional overturning circulation is, however, weaker in JJA than in DJF, and larger in the regions of descent than in the region of ascent. When averaging between 5°S and 5°N, the contribution from the meridional overturning circulation is much stronger.

5. Conclusions

A firmer, more precise and unambiguous basis for the common and useful practice of partitioning of the three-dimensional tropical overturning circulation into the zonal and meridional circulations has been sought as, in the past, the methods used to partition these circulations have been mostly ad hoc. Using a simplified version of the ψ-vector method developed by *Keyser et al.* [1989], the atmospheric vertical motion was partitioned into a component associated with overturning in the zonal direction and a component associated with overturning in the meridional direction. The mass fluxes associated with these two components were called the local Walker circulation and the local Hadley circulation respectively. This analysis is based on the divergent circulation as it is associated with the vertical motion and hence, convection. The analysis focused on the period 1979 to 2009. Partitioning the three-dimensional overturning circulation into a pair of two-dimensional overturning circulations proved to be conceptually useful and allowed for the decomposition of the divergent circulations in the zonal and meridional plane not only globally, but in specific regions. However, as the local Hadley and local Walker circulations were diagnosed from the ERA-Interim Reanalysis, the results must be treated with some caution as the accuracy of the divergent part of the circulation is uncertain, especially in the tropics.

The spatial pattern of the time-mean local Hadley circulation comprises localized, zonally-elongated bands with mostly ascent in the tropics and mostly subsidence in the subtropics, although in the eastern Pacific the mass flux is downward along the equator and southwards into the extratropics. The regions of ascent are shifted towards the summer hemisphere, while the regions of subsidence were more marked in the winter hemisphere. The patterns of vertical mass flux comprising the time-mean local Walker circulation are mostly oriented meridionally. Almost everywhere, the time-mean local Hadley circulation is stronger, and its seasonal variation larger, than the corresponding time-mean local Walker circulation. During DJF, the time-mean local Walker circulation is strongest in the eastern Pacific and South America, with upward mass fluxes over the continent and downward mass fluxes over the adjacent ocean. The time-mean local Walker circulation is prominent also through Asia and eastern Africa during JJA.

The local Walker circulation is stronger during a La Niña and weaker during an El Niño, especially in the eastern Pacific. However, the local Hadley circulation responds more strongly to an El Niño than the local Walker circulation, suggesting that an El Niño cannot be interpreted as simply a zonal shift in the Walker circulation.

The Hadley and Walker circulations (as distinct from the local Hadley and local Walker circulations) are commonly defined as the zonal and meridional averages of the overturning circulation respectively. In defining the Walker circulation, the average is often defined over a restricted latitudinal band. It was shown that, in this case, the vertical mass flux includes a contribution from the meridional overturning circulation. Nonetheless, defining the Hadley circulation by averaging over a limited region introduces only small errors as the contribution from the zonal overturning circulation is small. In contrast, the Walker circulation should not generally be defined by averaging over a limited region, as the meridional overturning circulation contributes to the definition of the Walker circulation. To avoid this problem the regional Hadley and regional Walker circulations were defined as the meridional and zonal averages of the local Hadley and local Walker circulations respectively. The contribution from the meridional overturning circulation to the meridionally-averaged mass flux becomes even more acute when averaging between 5°S and 5°N instead of 35°S and 10°N. This emphasizes the dependance of the result on the partitioning of the vertical mass flux as well as the region of averaging.

As ENSO is associated with the largest interannual variability in the Pacific region we investigated the regional Hadley circulation over the Maritime Continent as well as the regional Walker circulations in each ocean basin during El Niño and La Niña phases. In DJF, the regional Hadley circulation over the Maritime Continent is stronger and the region of ascent is wider during La Niña than during El Niño. In JJA, the regional Hadley circulation is stronger during El Niño, although the cell in the Northern Hemisphere is weaker during El Niño than during La Niña. The cell of the regional Hadley circulation located in the Northern Hemisphere is relatively weak during both El Niño and La Niña.

In addition there is a double cell structure for the regional Hadley circulation in DJF and a single cell structure in JJA.

In DJF during an El Niño, the regional Walker circulation in the Pacific is characterized by the region of strongest ascent in the central Pacific. During a La Niña the ascent is shifted westwards although the magnitude remains unchanged. The descent is located over the eastern Pacific and becomes stronger during La Niña. Thus, the regional Walker circulation in the Pacific becomes wider. During El Niño the regional Walker circulation in the Pacific is relatively narrow, although it is still the largest regional Walker circulation. In the Indian Ocean, the regional Walker circulation is relatively weak with the largest descent west of the western Australian coast during La Niña. The regional Walker circulation in the Atlantic is narrow, but of similar intensity to that in the Pacific, and intensifies during La Niña. In JJA, the regional Walker circulation in the Indian Ocean is strongest, particularly during La Niña. The regional Walker circulation in the Pacific is stronger during La Niña but remains in roughly the same place with the main ascent in the western Pacific.

As a next step we will use the ψ-vector method to analyze trends in the regional Hadley and regional Walker circulations. We will also apply the ψ-vector method to decompose the quasi-geostrophic omega equation and to attribute the source terms of this equation to changes in the regional Hadley and regional Walker circulations.

Acknowledgments. This research was supported by the Australian Research Council Grant FS100100081. We would like to thank Roger Smith for his valuable comments on an earlier version of this manuscript.

References

Barry, R. G., and A. M. Carleton, *Synoptic and Dynamic Climatology*, 620 pp., Routledge, 2001.

Bell, G. D., and M. S. Halpert, Climate assesment for 1997, *Bull. Amer. Meteor. Soc.*, *79*, S1–S50, 1998.

Chen, J., B. Carlson, and A. Genio, Evidence for strengthening of the tropical general circulation in the 1990s, *Science*, *296*, 838–841, 2002.

Dee, D. P., et al., The ERA-Interim reanalysis: configuration and performance of the data assimilation system, *Q. J. R. Meteorol. Soc.*, *137*, 553–597, 2011.

Eliassen, A., On the vertical circulation in frontal zones, *Geophys. Publ.*, *24*, 147–160, 1962.

Gastineau, G., L. Li, and H. Le Treut, The Hadley and Walker circulation changes in global warming conditions described by idealized atmospheric simulations, *J. Climate*, *22*, 3993–4013, 2009.

Gill, A. E., Some simple solutions for heat-induced tropical circulation, *Q. J. R. Meteorol. Soc.*, *106*, 447–462, 1980.

Goswami, B. N., V. Krisnamurthy, and H. Annamalai, A broadscale index for the interannual variability of the Indian summer monsoon, *Q. J. R. Meteorol. Soc.*, *125*, 611–633, 1999.

Hagos, S., and L. R. Leung, On the relationship between uncertainties in tropical divergence and the hydrological cycle in global model, *J. Climate*, *25*, 381–391, 2012.

Hagos, S., and C. Zhang, Diabatic heating, divergent circulation and moisture transport in the African monsoon system, *Q. J. R. Meteorol. Soc.*, *136(s1)*, 411–425, 2010.

Hartmann, D., *Global Physical Climatology*, 411 pp., Academic Press, 1994.

Held, I. M., and A. Y. Hou, Nonlinear axially symmetric circulations in a nearly inviscid atmosphere, *J. Atmos. Sci.*, *37*, 515–533, 1980.

Holton, J. R., *An introduction to dynamic meteorology*, 415-419 pp., 4th ed. Elsevier Academic Press, 2004.

Hu, Y., and Q. Fu, Observed poleward expansion of the Hadley circulation since 1979, *Atmos. Chem. Phys.*, *7*, 5229–5236, 2007.

James, I. N., *Introduction to Circulating Atmospheres*, 93-97 pp., Cambridge Atmospheric and Space Science Series, 1994.

Julian, P. R., and R. M. Chervin, A study of the Southern Oscillation and the Walker circulation phenomenon, *Mon. Wea. Rev.*, *106*, 1433–1451, 1978.

Kang, S., and J. Lu, Expansion of the Hadley cell under global warming: Winter versus summer, *J. Climate*, *25*, 8387–8393, 2012.

Keyser, D., B. D. Schmidt, and D. G. Duffy, A technique for representing three-dimensional vertical circulations in baroclinic disturbance, *Mon. Wea. Rev.*, *117*, 2463–2494, 1989.

Keyser, D., B. D. Schmidt, and D. G. Duffy, Quasigeostrophic diagnosis of three–dimensional ageostrophic circulations in an idealized baroclinic disturbance, *Mon. Wea. Rev.*, *120*, 698–730, 1992.

Krishnamurthy, V., and B. N. Goswami, Indian monsoon - ENSO relationship on inter-decadal timescale, *J. Clim.*, *13*, 579–595, 2000.

Kumar, K., B. Rajgopalan, and M. Cane, On the weakening relationship between the Indian monsoon and ENSO, *Science*, *284*, 2156–2159, 1999.

L'Heureux, M. L., S. Lee, and B. Lyon, Recent multidecadal strengthening of the Walker circulation across the tropical Pacific, *Nature Climate.*, p. doi:10.1038/NCLIMATE1840, 2013.

Loughe, A. F., C.-C. Lai, and D. Keyser, A technique for diagnosing three-dimensional ageostrophic circulations in baroclinic disturbances on limited-area domains, *Mon. Wea. Rev.*, *123*, 1476–1504, 1995.

Lu, J., G. A. Vecchi, and T. Reichler, Expansion of the Hadley cell under global warming, *Geophy. Res. Lett.*, *34*, doi: 10.1029/2006GL028,443, 2007.

Mitas, C. M., and A. Clement, Has the Hadley cell been strengthening in recent decades?, *Geophys. Res. Lett.*, *32*, doi:10.1029/2004GL021,765, 2005.

Moore, G. W. K., K. Alverson, and G. Holdsworth, Mount Logan ice core evidence for changes in the Hadley and Walker circulations following the end of the Little Ice Age, in *Chapter 13, The Hadley Circulation: Present, Past and Future*, edited by H. F. Diaz and R. S. Bradley, pp. 371–395, Kluwer Acadamic Publishers, 2004.

Oort, A., and J. Yienger, Observed interannual variability in the Hadley circulation and its connection to ENSO, *J. Climate*, *9*, 2751–2767, 1996.

Power, S., and I. Smith, Weakening of the Walker Circulation and apparent dominance of El-Nino both reach record levels, but has ENSO really changed?, *Geophy. Res. Lett.*, *34*, doi:10.1029/2007GL030,854, 2007.

Quan, X., H. Diaz, and M. Hoerling, Changes in the Tropical Hadley cell since 1950, in *Chapter 3, The Hadley Circulation: Present, Past and Future*, edited by H. F. Diaz and R. S. Bradley, pp. 85–120, Kluwer Acadamic Publishers, 2004.

Reeder, M. J., D. Keyser, and B. D. Schmidt, Three-dimensional baroclinic instability and summertime frontogenesis in the Australian region, *Q. J. R. Meteorol. Soc.*, *117*, 1–28, 1991.

Seidel, D. N., Q. F. amd W. J. Randel, and J. Reichler, Widening of the tropical belt in a changing climate, *Nature Geoscience*, *1*, 21–24, 2008.

Simmons, A., S. Uppala, D. Dee, and S. Kobayashi, New ECMWF reanalysis products from 1989 onwards, *ECMWF Newsletter*, *110*, 26–35, 2011.

Stachnik, J. P., and C. Schumacher, A comparison of the Hadley circulation in modern reanalyses, *J. Geophys. Res.*, *116*, doi:10.1029/2011JD016,677, 2011.

Tanaka, H., N. Ishizaki, and A. Kitoh, Trend and interannual variability of Walker, Monsoon and Hadley circulations defined by velocity potential in the upper troposphere, *Tellus*, *56*, 250–269, 2004.

Tokinaga, H., S.-P. Xie, C. Deser, Y. Kosaka, and Y. M. Okumura, Slowdown of the Walker circulation driven by tropical Indo-Pacific warming, *Nature*, *491*, 439–443, 2012.

Trenberth, K., and D. Stepaniak, Seamless poleward atmospheric energy transports and implications for the Hadley circulation, *J. Climate*, *16*, 3706–3722, 2003.

Trenberth, K., D. Stepaniak, and J. Caron, The global monsoon as seen through the divergent atmospheric circulation, *J. Climate*, *13*, 3969–3993, 2000.

Vecchi, G., B. Soden, A. Wittenberg, I. Held, A. Leetmaa, and M. Harrison, Weakening of tropical Pacific atmospheric circulation due to anthropogenic forcing, *Nature*, *441*, 73–76, 2006.

Wang, C., Atlantic climate variability and its associated atmospheric circulation cells, *J. Climate*, *15*, 1516–1536, 2002.

Webster, P. J., and S. Yang, Monsoon and ENSO: Selectively interactive systems, *Q. J. R. Meteorol. Soc.*, *118*, 877–926, 1992.

Yu, B., and W. Zwiers, Changes in equatorial atmospheric zonal circulations in recent decades, *Geophys. Res. Lett.*, *37*, doi:10.1029/2009GL042,071, 2010.

Zhao, H., and G. Moore, Trends in the boreal summer regional Hadley and Walker circulations as expressed in precipitation records from Asia and Africa during the latter half of the 20th Century, *Int. J. Climatol.*, *28*, 563–578, 2008.

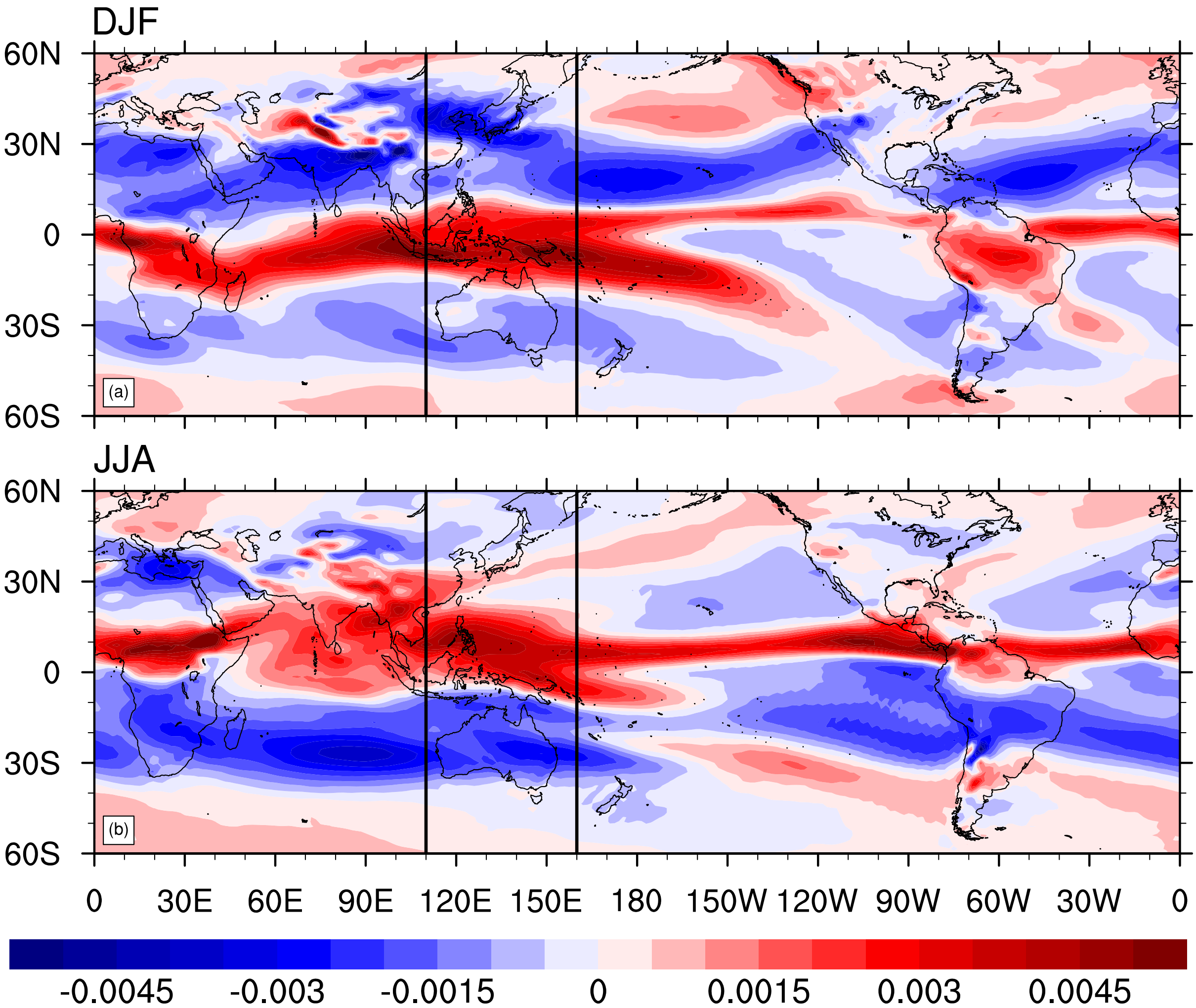

Figure 1. The local Hadley circulation. The meridional mass flux ($\mathrm{kg\,m^{-2}\,s^{-1}}$) at 500 hPa calculated from the ERAI reanalysis (1979 - 2009) for the seasons (a) DJF and (b) JJA is shown in shadings of red (ascent) and blue (descent). The black lines at 110°E and 160°E mark the area defining the regional Hadley circulation over the Maritime Continent.

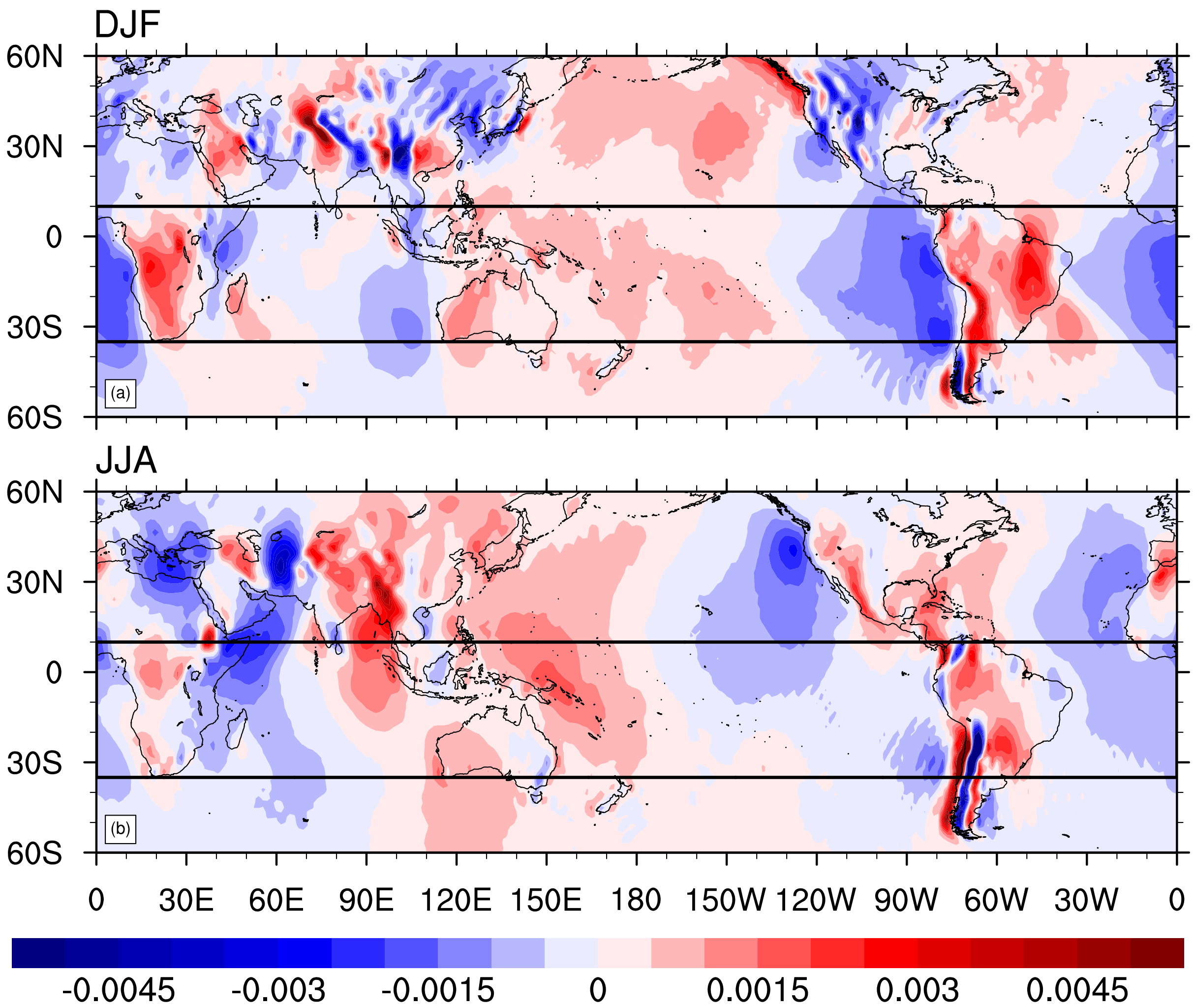

Figure 2. The local Walker circulation. The zonal mass flux ($\mathrm{kg\,m^{-2}\,s^{-1}}$) at 500 hPa calculated from the ERAI reanalysis (1979 - 2009) for the seasons (a) DJF and (b) JJA. The box shown (0-360°, 10°N-35°S) marks the area defining the regional Walker circulations.

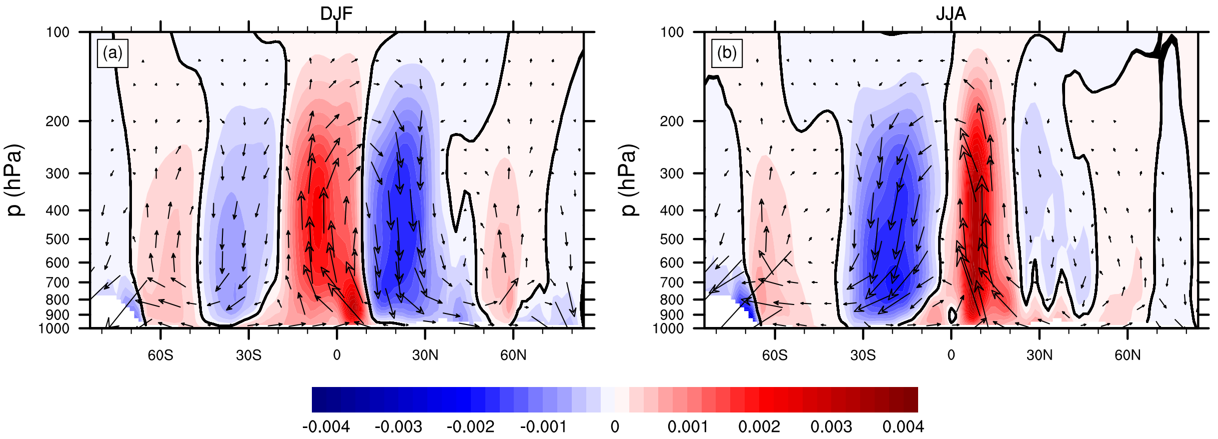

Figure 3. The Hadley circulation from the ERAI reanalysis (1979 - 2009) for (a) DJF and (b) JJA. The vertical mass flux in meridional direction ($[m_\phi]$, $\mathrm{kg\,m^{-2}\,s^{-1}}$) is shaded. Vectors represent the wind in the plane of the cross section ($[u_\phi], [\omega_\phi]$). The zero value of $[m_\phi]$ is displayed as a thick black line. Fields below the mean orography are omitted.

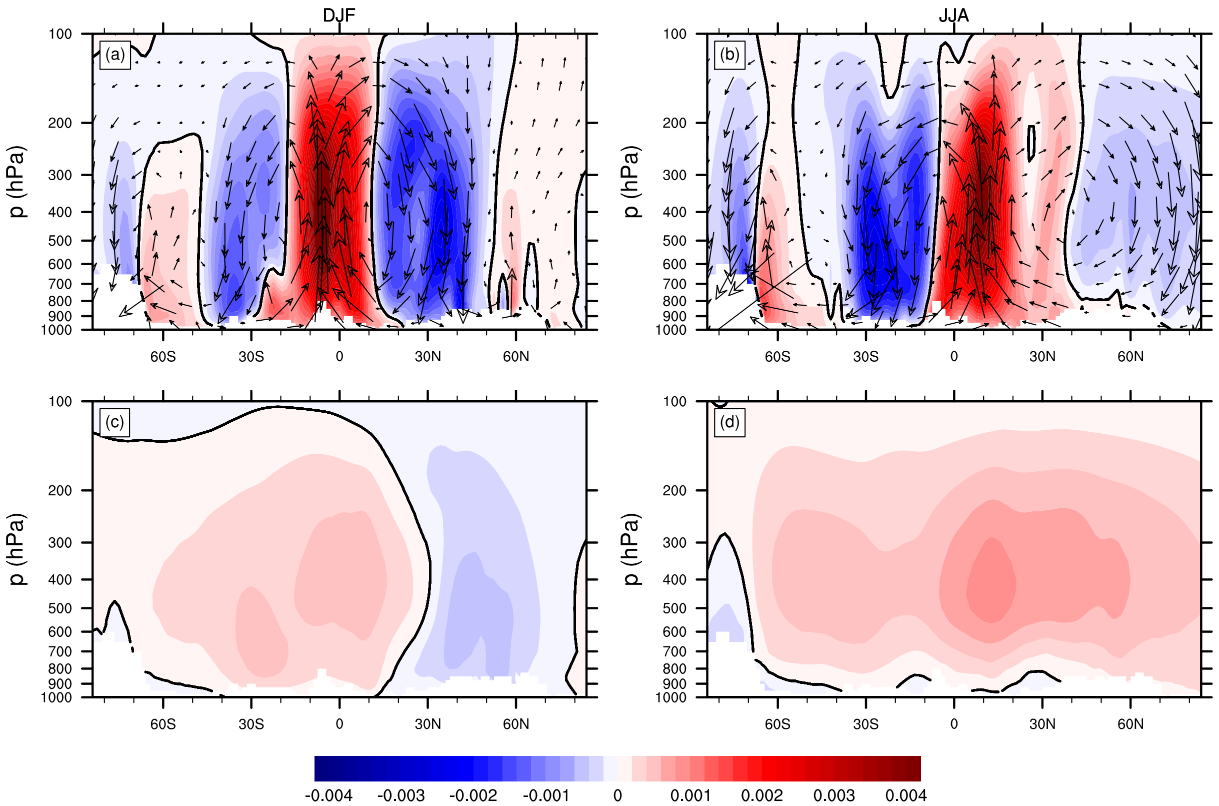

Figure 4. The regional Hadley circulation over the Maritime Continent (region shown in Fig. 1) from the ERAI reanalysis (1979 - 2009) for (a) DJF and (b) JJA averaged over the longitudes 110 °E to 160 °E. The vertical mass flux in the meridional plane ($[m_\phi]^{160°E}_{110°E}$, $\mathrm{kg\,m^{-2}\,s^{-1}}$) is shaded. Vectors represent the wind in the plane of the cross section ($[u_\phi]^{160°E}_{110°E}$, $[\omega_\phi]^{160°E}_{110°E}$). The contribution to the vertical mass flux from the zonal overturning circulation ($[m_\lambda]^{160°E}_{110°E} = [m]^{160°E}_{110°E} - [m_\phi]^{160°E}_{110°E}$, $\mathrm{kg\,m^{-2}\,s^{-1}}$) for (c) DJF and (d) JJA is shaded. The zero value of the respective variable is displayed as a thick black line. Fields below the maximum orography are omitted.

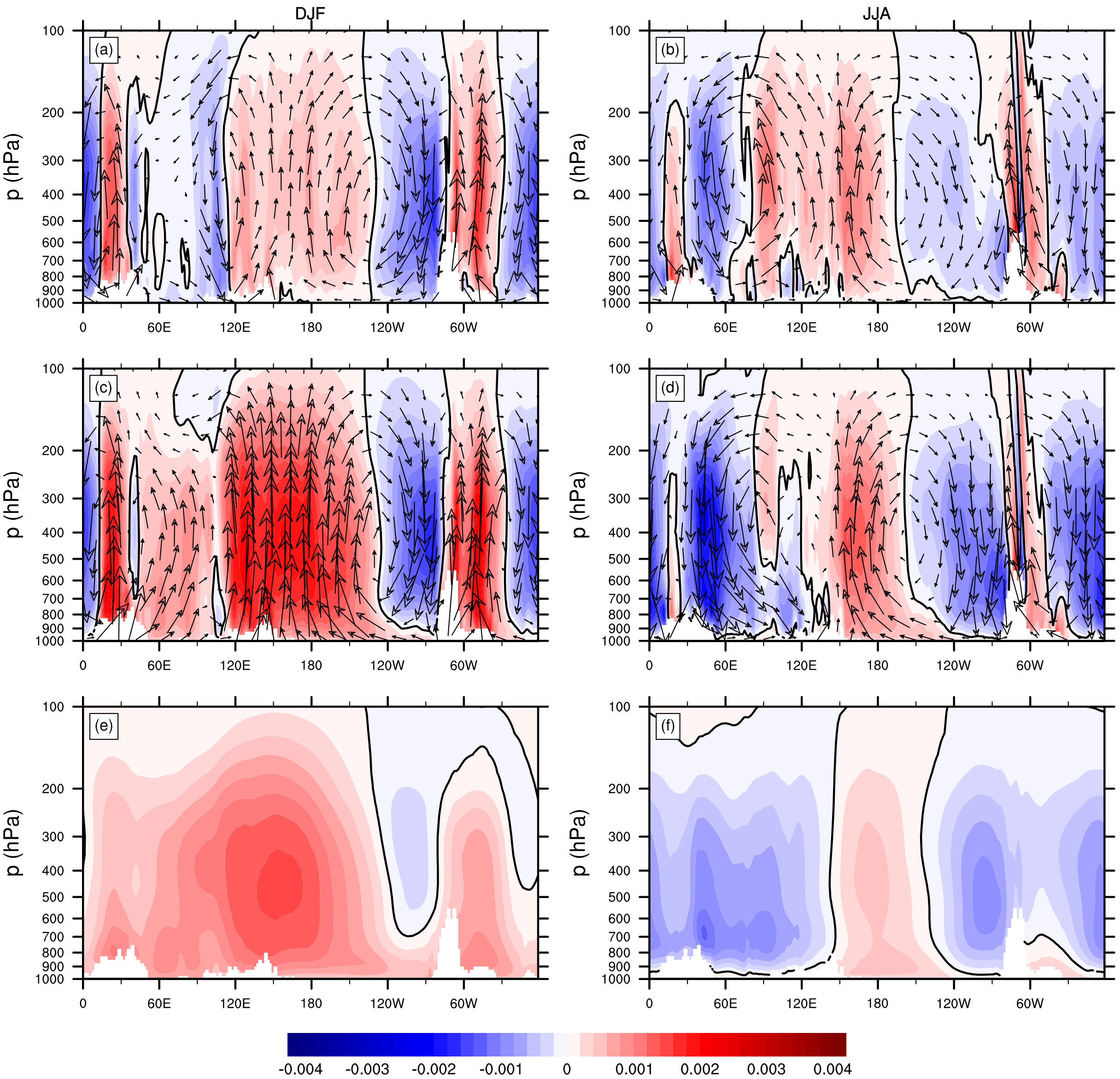

Figure 5. The regional Walker circulation (region shown in Fig. 2) from the ERAI reanalysis (1979 - 2009) for (a) DJF and (b) JJA averaged over the latitudes 35 °S to 10 °N. The vertical mass flux in the zonal plane ($< m_\lambda >^{10°N}_{35°S}$, $\mathrm{kg\,m^{-2}\,s^{-1}}$) is shaded. Vectors represent the wind in the plane of the cross section ($< u_\lambda >^{10°N}_{35°S}, < \omega_\lambda >^{10°N}_{35°S}$). The vertical mass flux ($< m >^{10°N}_{35°S}$, $\mathrm{kg\,m^{-2}\,s^{-1}}$) is shaded for (c) DJF and (d) JJA. Vectors represent the wind in the plane of the cross section ($< u_\lambda >^{10°N}_{35°S}, < \omega >^{10°N}_{35°S}$). The contribution to the vertical mass flux from the meridional overturning circulation $< m_\phi >^{10°N}_{35°S} = < m >^{10°N}_{35°S} - < m_\lambda >^{10°N}_{35°S}$ ($\mathrm{kg\,m^{-2}\,s^{-1}}$) is shaded for (e) DJF and (f) JJA. The zero value of the respective fields is displayed as a thick black line. Fields below the maximum orography are omitted.

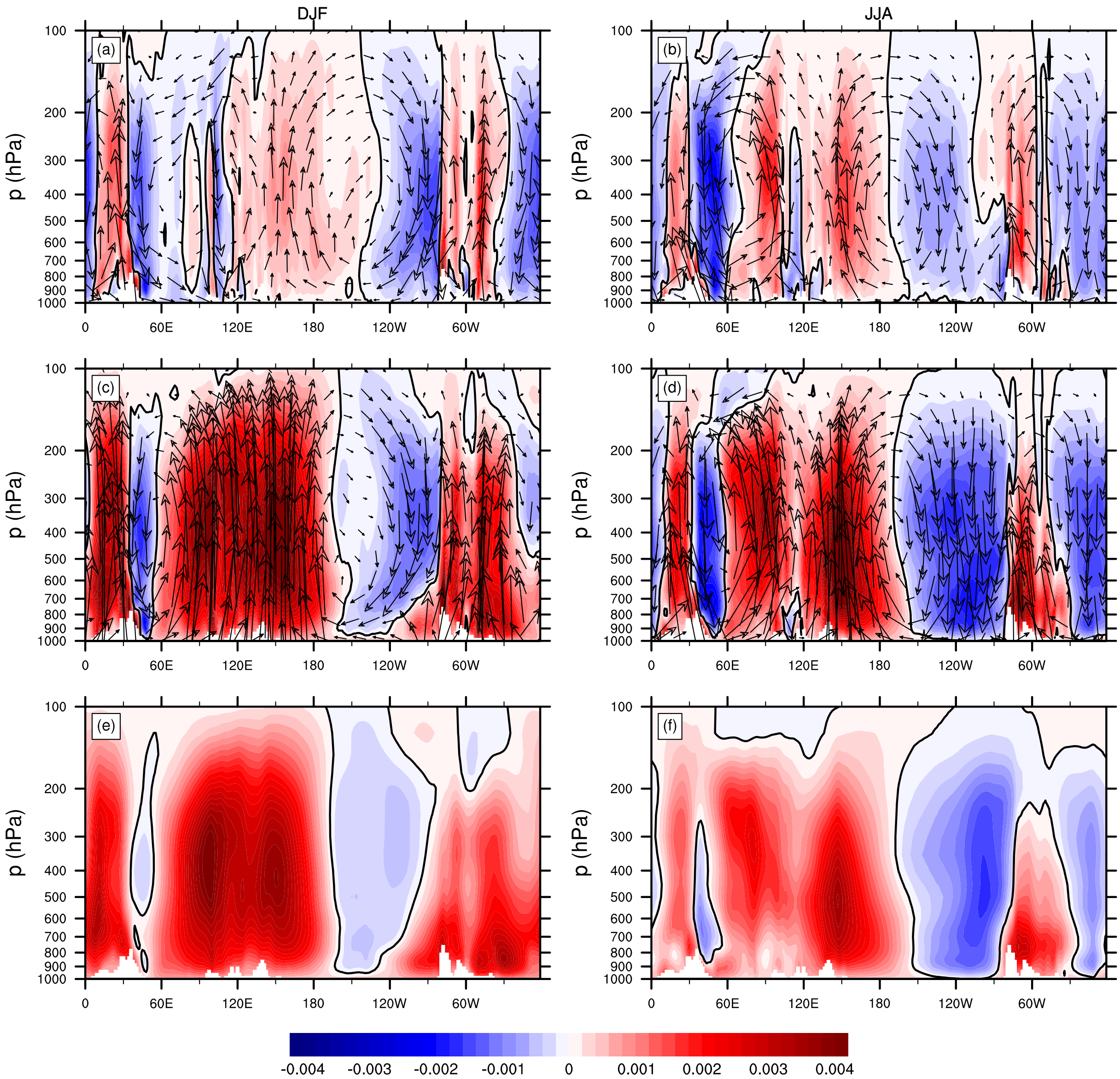

Figure 6. The same as Fig. 5, but meridionally averaged between 5°S and 5°N.

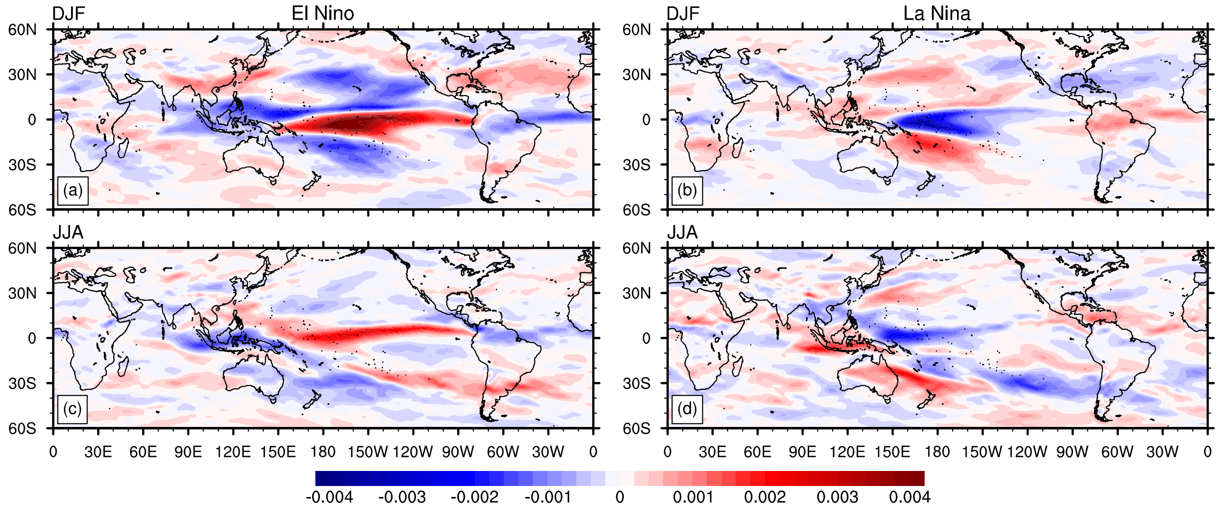

Figure 7. Anomalies of the local Hadley circulations at 500 hPa with respect to the mean for 1979-2009. The anomalies in the meridional mass flux m_ϕ ($\mathrm{kg\,m^{-2}\,s^{-1}}$) for El Niño (left) and La Niña (right) periods are shown for DJF (top row) and JJA (bottom row).

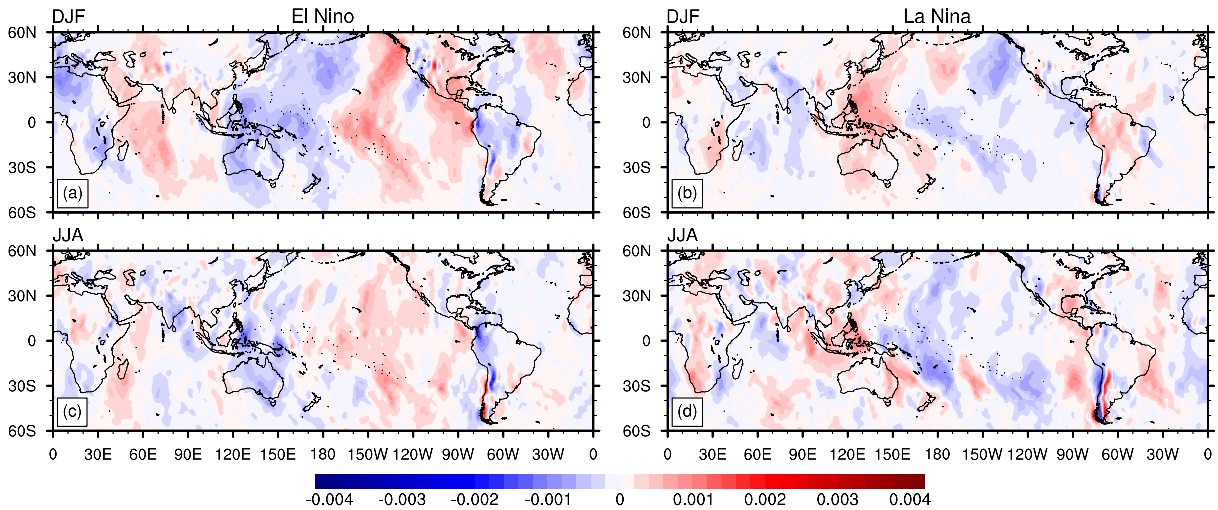

Figure 8. Anomalies of the local Walker circulation at 500 hPa with respect to the mean for 1979-2009. The anomalies in the zonal mass flux m_λ ($\mathrm{kg\,m^{-2}\,s^{-1}}$) for El Niño (left) and La Niña (right) periods are shown for DJF (top row) and JJA (bottom row).

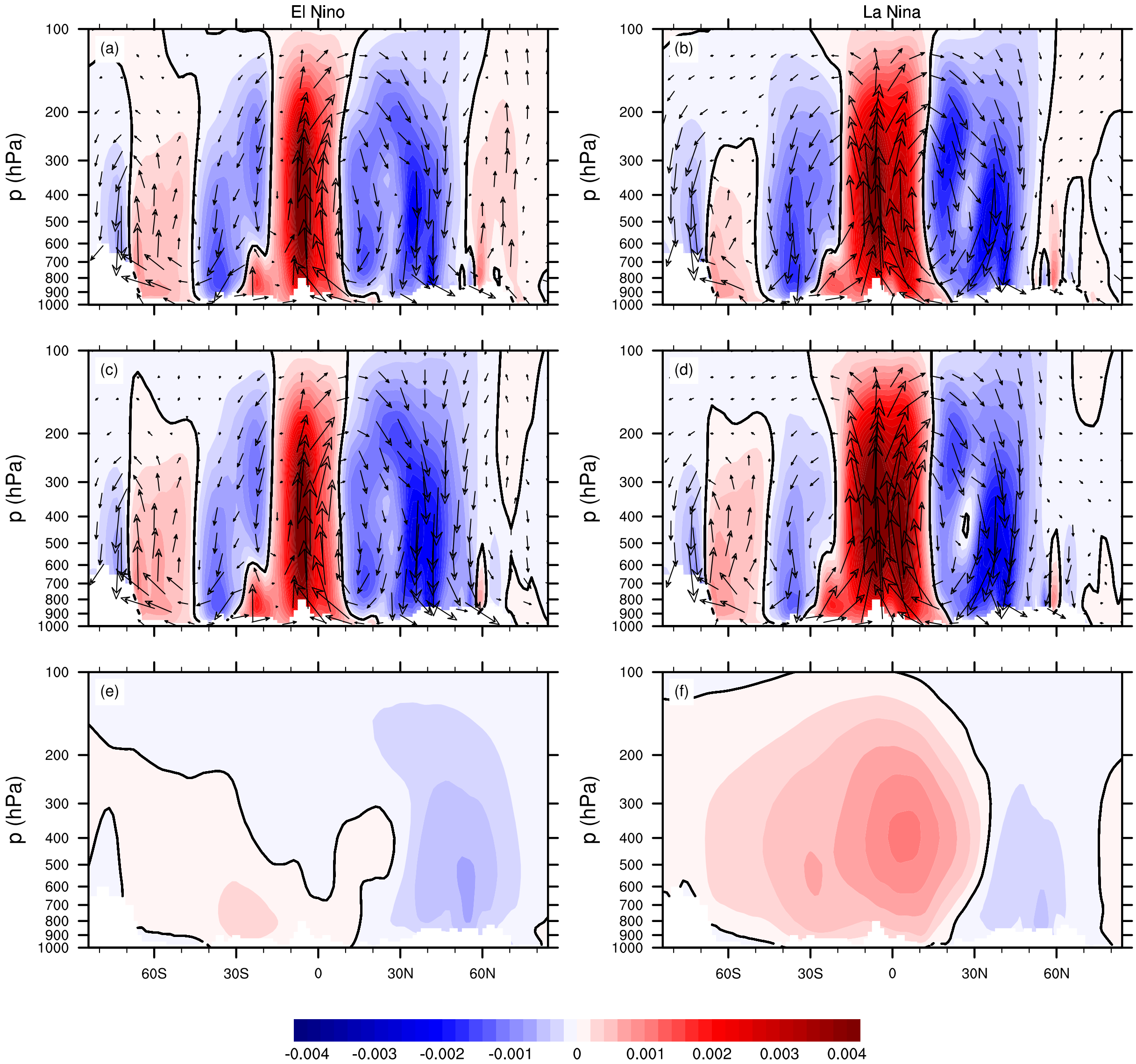

Figure 9. The regional Hadley circulation for the Maritime Continent (see box in Fig. 1) during El Niño (left) and La Niña (right) periods in DJF calculated from the ERAI reanalysis (1979 - 2009) averaged over the longitudes 110 °E to 160 °E. (a), (b): The regional Hadley circulation ($[m_\phi]_{110^\circ E}^{160^\circ E}$, $\mathrm{kg\,m^{-2}\,s^{-1}}$) is shaded, and the wind in the plane of the cross section ($[u_\phi]_{110^\circ E}^{160^\circ E}$, $[\omega_\phi]_{110^\circ E}^{160^\circ E}$). (c), (d): The vertical mass flux ($[m]_{110^\circ E}^{160^\circ E}$, $\mathrm{kg\,m^{-2}\,s^{-1}}$) is shaded, and the wind in the plane of the cross section ($[u_\phi]_{110^\circ E}^{160^\circ E}$, $[\omega]_{110^\circ E}^{160^\circ E}$). (e), (f): The contribution of the zonal overturning circulation ($[m_\lambda]_{110^\circ E}^{160^\circ E}$, $\mathrm{kg\,m^{-2}\,s^{-1}}$) to the vertical mass flux is shaded. In all plots the zero-line is displayed as a thick black line. The maximum orography in this box is masked out.

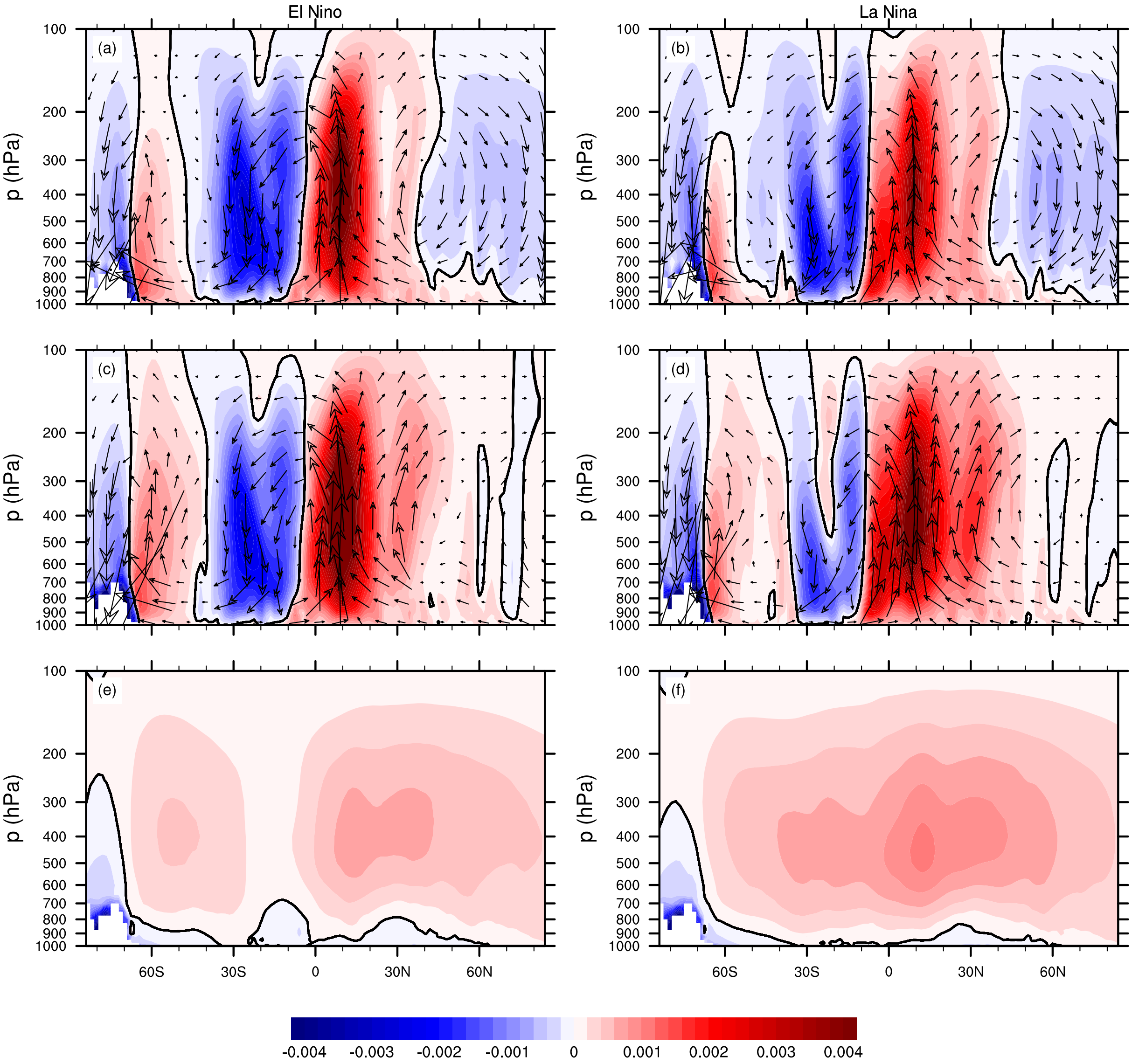

Figure 10. The same as Fig. 9, but for JJA.

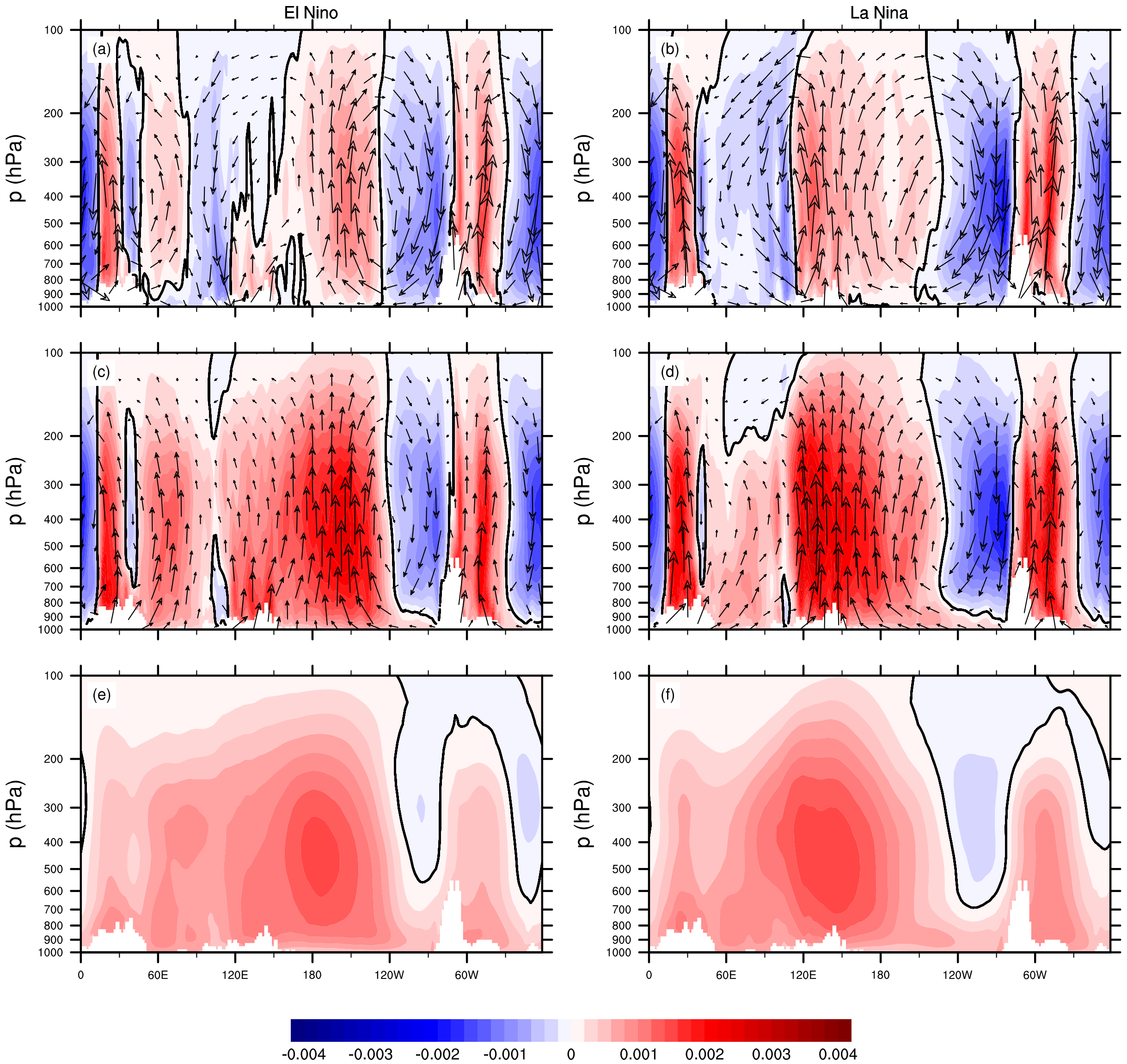

Figure 11. The regional Walker circulation for El Niño (left) and La Niña (right) periods in DJF calculated from the ERAI reanalysis (1979 - 2009) averaged over the latitudes 35 °S to 10 °N. (a), (b): The vertical mass flux in the zonal plane ($< m_\lambda >_{35^\circ S}^{10^\circ N}$, $\mathrm{kg\,m^{-2}\,s^{-1}}$) is shaded, and the wind in the plane of the cross section ($< u_\lambda >_{35^\circ S}^{10^\circ N}, < \omega_\lambda >_{35^\circ S}^{10^\circ N}$). (c), (d): The vertical mass flux ($< m >_{35^\circ S}^{10^\circ N}$, $\mathrm{kg\,m^{-2}\,s^{-1}}$) is shaded, and the wind in the plane of the cross section ($< u_\lambda >_{35^\circ S}^{10^\circ N}, < \omega >_{35^\circ S}^{10^\circ N}$). Note, the magnitude of the wind vectors is double the magnitude of the wind vectors shown in (a) and (b). (e), (f): The contribution from the meridional circulation ($< m_\phi >_{35^\circ S}^{10^\circ N}$, $\mathrm{kg\,m^{-2}\,s^{-1}}$) to the mass flux is shaded. In all plots the zero-line is displayed as a thick black line. The maximum orography in this box is masked out.

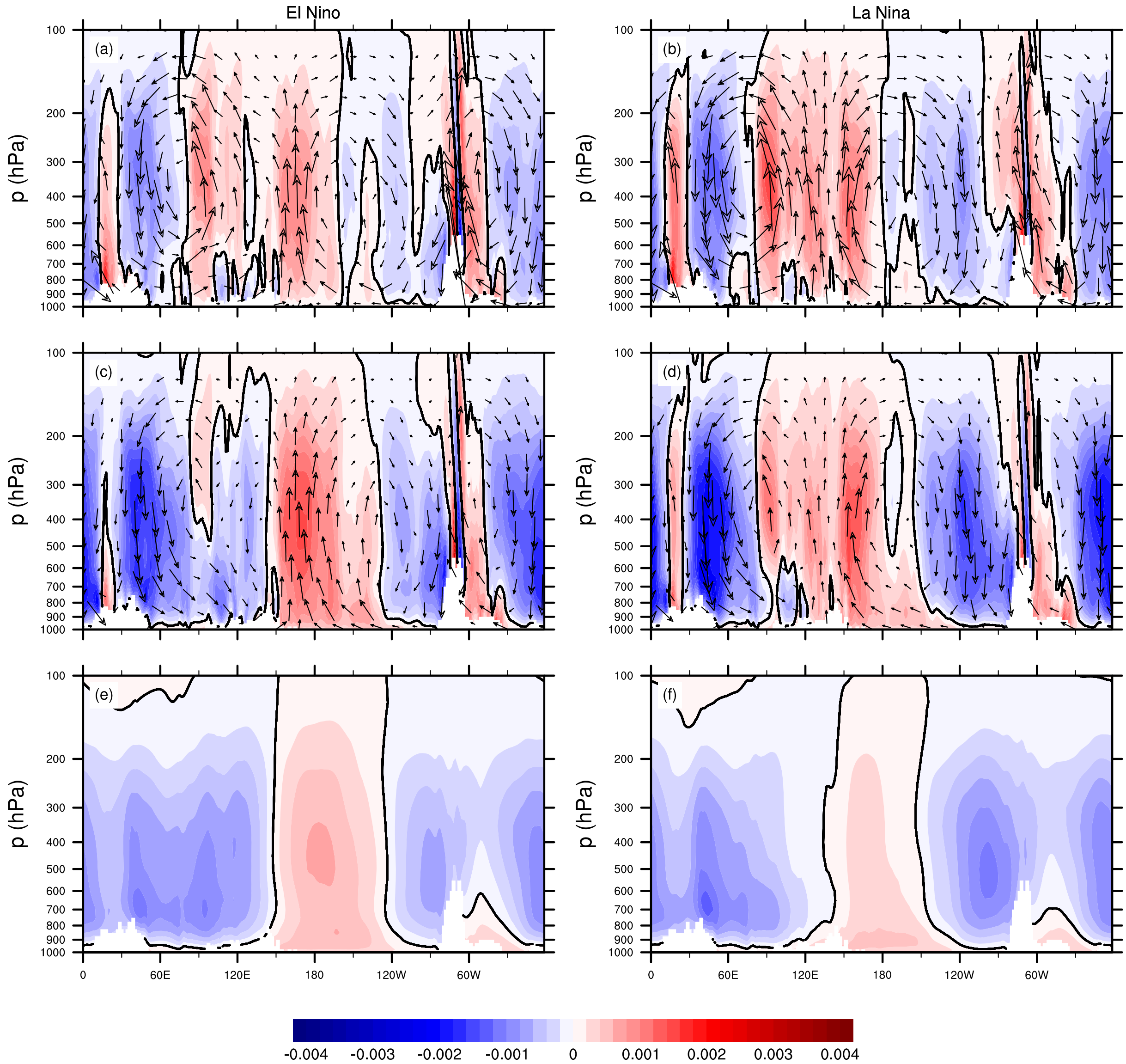

Figure 12. The same as Fig. 11, but for JJA, except the wind vectors all have the same reference vector.